Iranian Journal of Science and Technology, Transactions of Mechanical Engineering
https://doi.org/10.1007/s40997-024-00762-1

RESEARCH PAPER

Cooling and Tribological Performance Analyses of a Refrigeration System Using Nano-Fluids as Refrigerant and Lubricant

Ali Can Yilmaz[1] · **Ahmet Cosgun**[2]

Received: 20 December 2023 / Accepted: 25 February 2024
© The Author(s), under exclusive licence to Shiraz University 2024

Abstract

This experimental study investigates the effects of TiO_2 nano-particles on the cooling and tribological performance of a vapor compression refrigeration system running on R134a as refrigerant and polyolester oil (POE) as lubricant. Dynamic light scattering analysis was conducted to observe the dispersion of the nano-particles. The heat transfer rate in the evaporator and condenser was taken into consideration to observe the cooling performance of the system charged with combination of 0.1 vol% and 0.5 vol% TiO_2 incorporated nano-refrigerants (R0.1 & R0.5) and 0.1 vol% and 0.5 vol% TiO_2 incorporated POE nano-lubricants (P0.1 & P0.5). Coefficient of friction and wear rate analyses were also performed on the piston ring of the compressor by immersing the samples in two different lubricants (P0.1 & P0.5). The compressor's suction-discharge characteristics were assessed to determine the impact of the nano-fluid combinations. Scanning electron microscopy was used to examine the morphology of the nano-particles and worn surfaces. Atomic force microscopy was utilized to observe the structure of the worn substrates. The chemical composition of the worn surfaces was analyzed using energy-dispersive X-ray and the thermal stability of the nano-additives was ascertained via thermogravimetric analysis and differential scanning calorimeter. The best cooling and tribological performance results were obtained when the system was run on a combination of R0.5 + P0.1. Compared to standard conditions (R134a + POE), the highest increase in COP was 35.86% for R0.5 + P0.1. With the same combination, the cooling time was reduced by 22.25% and the highest decrease in the average coefficient of friction was 8.02% for 0.1 vol% of TiO_2 incorporated POE lubricant (P0.1).

Keywords Refrigeration system · Heat transfer · COP · TiO_2 nano-particles · Tribological performance

Abbreviations

POE	Polyolester oil
COP	Coefficient of performance
CW	Compressor work
SDBS	Sodium dodecyl benzene sulfonate
CFD	Computational fluid dynamics
VCRS	Vapor compression refrigeration system
SEM	Scanning electron microscopy
AFM	Atomic force microscopy
EDX	Energy-dispersive X-ray
DSC	Differential scanning calorimeter
TGA	Thermo-gravimetric analysis
DLS	Dynamic light scattering
ξ_{max}	Maximum of the measured parameter
RSM	Response surface methodology
FCCD	Face-centered central composite design
ANOVA	Analysis of variance

List of Symbols

q	Heat release rate (kW)
Re	Reynold's number
r	Distance between point of observation and particle (m)
m	Mass (g)
c	Specific heat capacity (J/kg °C)
K	Energy meter constant (impulse/kWh)
t	Time lapse (h)
T	Temperature (°C)
A	Trace area (mm^2)
L	Distance covered by the scratcher (mm)
Pe	Peclet number
P0.1, P0.5	0.1 Vol% TiO_2 nano-particle incorporated lubricant, 0.5 vol% TiO_2 nano-particle incorporated lubricant

✉ Ali Can Yilmaz
acyilmaz@cu.edu.tr

[1] Department of Motor Vehicles and Transportation Technologies, Cukurova University, 01160 Adana, Turkey

[2] Department of Mechanical Engineering, Akdeniz University, 07058 Antalya, Turkey

Published online: 26 March 2024

Pr	Prandtl number
D	Diameter (m)
u	Velocity (m/s)
Nu	Nusselt number
F	Normal load (N)
h	Convection heat transfer coefficient (W/m^2K)
V	Volume (m^3)
Q	Heat flux (W/m^2)
k	Thermal conductivity (W/mK)
D	Diameter (m)
u	Velocity (m/s)
R0.1, R0.5	0.1 Vol% TiO_2 nano-particle incorporated refrigerant, 0.5 vol% TiO_2 nano-particle incorporated refrigerant

Greek Letters

μ_a	Average coefficient of friction
ψ	Wear rate (mm^3/Nm)
Γ	Dispersed light intensity (cd)
Λ	Light wavelength (m)
Φ	Medium refractive index ratio
β	Angle between the directions of the incident and the scattered lights (°)
Ζ	Zeta potential (mV)
σ	Standard deviation
ρ	Density (kg/m^3)
υ	Electrophoretic mobility (μm.cm/Vs)
η	Liquid viscosity (Pa.s)
ε	Dielectric constant
ε_0	Permittivity of free space (F/m)
ξ_{max}	Maximum of the measured parameter
Σ	Percentage error
ℓ	Measurement range
τ	Sphericity
α	Thermal diffusivity (m^2/s)

1 Introduction

Any refrigeration system that uses nano-refrigerant instead of traditional refrigerant is intended to be more lightweight, compact and efficient. These refrigeration systems have lower power consumption and are therefore more energy-efficient. The reason for this is that nano-refrigerants have better thermo-physical characteristics than conventional refrigerants (Kundan 2021).

Nano-sized particles (1–100 nm) dispersed in base fluids composes the advanced class of fluids known as "nano-fluids" (Prasad et al. 2017). They are usually composed of metals (Ghalme et al. 2020; Choi et al. 2009; Thottackkad et al. 2012; Kong et al. 2017), nonmetals (Peng et al. 2009a; Kane et al. 2016; Sanukrishna et al. 2019), or their oxides (Mousavi and Heris 2020; Yang et al. 2021), nano-particles have the ability to enhance the base fluids' conduction and convection thermal performance (Putra et al. 2003).

Heat is absorbed in the evaporator and rejected in the condenser as the refrigerant fluid in a system flows through it, undergoing constant phase shifts. The measure of a system's cooling performance known as the coefficient of performance (COP) is the ratio of the evaporator's heat release rate (q) to the compressor's work (CW) (Sabareesh et al. 2012):

$$COP = \frac{q}{CW} \tag{1}$$

Enhancing heat release rate can increase a system's COP, and metallic nano-particles are widely known for having excellent heat transfer capabilities. Jin et al. (2023) investigated the effects of addition of TiO_2 nano-particles to absorption refrigeration system using NH_3-H_2O–LiBr as working fluid. They concluded that the maximum improvement in absorption efficiency and COP were 85% and 13.7%, respectively. Jiang et al. (2019) built a miniaturized ammonia–water absorption refrigeration system to investigate the influence of the different amounts of TiO_2 nano-particles on COP of the system along with sodium dodecyl benzene sulfonate (SDBS) as dispersant. They achieved an increment of up to 27% in COP when the system is run on the mixture of 0.5 wt% TiO_2 and the 0.02 wt% SDBS. Another experimental study related to performance of a heat pump using R22 + TiO_2 as working fluid was conducted by Li et al. (2015). They deduced that for the heating cycle of the heat pump system, COP increment could be up to 80% when the system is charged with R22 + TiO_2 nano-particles by weight ratio of 5%. On the other hand, there are intriguing studies i.e. on effects of nano-fluids on performance improvement of magnetic regenerators (Scarpa and Bianco 2024), photovoltaic thermoelectric air conditioner (Bakthavatchalam et al. 2022) and heat exchangers (Liu et al. 2022).

Heat transfer analysis across the refrigeration system is of great importance in terms of heat transfer performance. Mahbubul et al. (2015) incorporated 5 vol.% Al_2O_3 nano-particles in R134a refrigerant at temperatures of 283–308 K at a uniform mass flux. The results depicted a maximum of 28.58% enhancement of thermal conductivity for the nano-refrigerant compared to the base refrigerant. Mohamadi et al. (2021) conducted a theoretical study focusing on heat transfer characteristics and entropy generation analysis of a laminar nano-fluid flow in a 3 mm horizontal circular tube using ANSYS Fluent. They analyzed Al_2O_3 and SiO_2 nano-particles dispersed in HFE7000 in terms of mean pressure drop and entrophy generation at various volumetric concentrations and Reynolds numbers. They concluded that total entropy generation was diminished by approximately 20% when utilizing a sliding wall pipe with a slip length of 100 μm and 6% volume concentration of Al_2O_3 scattered in

HFE7000 as opposed to pure HFE7000 flowing in a no-slip pipe. Sheikholeslami et al. (2019) employed a refrigeration system with flattened channels in which the nano-refrigerant (R600a/oil/CuO) flows and investigated the influence of flattened percentage, flow rate, vapor quality and mass fraction of CuO on boiling heat transfer. An improvement in boiling heat transfer coefficient was obtained when the system was charged with nano-refrigerant. Other related studies can be found in (Mahbubul et al. 2013; Ghorbani et al. 2017; Fazlin et al. 2020).

Studies related to influence of nanoparticles on heat transfer behavior of thermodynamic systems have also undergone re-orientation towards optimization of the system using computational fluid dynamics (CFD) along with numerical methods. Abolpour and Shamsoddini (2023) presented a method of obtaining optimum mixture of Al_2O_3, Fe_2O_3, SiO_2, TiO_2, CuO, and ZnO nanoparticles in the heat exchanger to improve performance and provide low-pressure drop. In the first stage, they simulated a turbulent flow in CFD and developed a numerical method to solve the required equations. In the second stage of the study, they used genetic algorithm approach to optimize the amount of related nano-particles in the heat exchanger. Referring to the findings, the optimum combination of the nano-particles (4.48 vol%) results in 1.6% reduction and 14.94% increment in fluid entalphy change and mean pressure change, respectively. Khan and Amirtham (2023) conducted a theoretical analysis of a flat plate solar collector operating on TiO_2–Ag/water nano-fluid in terms of energy and exergy. They developed a regression model for 0.1 vol% and 0.2 vol% nano-particle concentrations in distilled water. The results depicted that nanoparticle concentration of 0.2 vol% is the optimum amount resulting in up to 18% improvement in thermal conductivity of the solar collector. Akcay and Akdag (2023) attempted to investigate the impact of Reynolds number (Re), pulsating amplitude (A) and Womersley number (Wo) on heat transfer behavior of a cam-shaped tube bundle in which CuO-water nano-fluid flows. They used ANSYS Fluent to carry out numerical solutions and the results depicted that pulsating frequency (Wo) over 14 has negative effect on heat transfer characteristics. Mohammadi (2023) made a numerical investigation regarding optimization of a heat exchanger filled with nano-fluid using 90 scenarios encompassing six design parameters such as various fin dimensions and different operating conditions of carrier flow using response surface methodology (RSM) based on the face-centered central composite design (FCCD). He developed regression models through analysis of variance (ANOVA) and concluded that 4000, 0.154 and 9.84 are the optimum values for Re, fin height/outer tube diameter and fin pitch/outer tube diameter, respectively. Shammasi et al. (2023) compared the Eulerian two-fluid model with single-phase model and mixing of these two in terms of convection heat transfer performance in a square cavity filled with Al-water nano-fluid in volume fractions of 0.1%, 0.3%, 1% and 2%. They showed that Eulerian model gives more accurate results than those of others and heat transfer and Nusselt number were prone to decrease at nano-particle fractions above 0.3 vol%.

Another method of raising a system's COP is to reduce compressor work (CW). Thanks to superior tribological properties of nano-particles in mechanical systems, nano-lubricants step forward in the context of reducing compressor work. In an experimental study, Sabareesh et al. (2012) investigated the enhancement of COP in a vapor compression refrigeration system through the dispersion of TiO_2 nano-particles in the compressor lubricant. According to their findings, a mere 0.01% volume fraction of TiO_2 nano-particles in the lubricant was adequate to increase the system's COP by 17% and decrease the compressor's work by roughly 11%. The performance evaluation of fullerene nano-particles in refrigeration mineral oil at concentrations of 0.01 vol% and 0.1 vol% was studied by Lee et al. (2009). It was estimated that a mere 0.1 vol% addition of fullerene to the lubricant can result in a 90% reduction in the coefficient of friction and a decrease in compressor work. ZnO nano-particles were added by Kumar and Singh (2017) to a refrigeration system using compressor lubricant and R290/R600a refrigerant. According to their findings, adding ZnO nano-particles at a mass fraction of 0.1% reduced the compressor's suction-discharge temperature and pressure values while saving 7.5% of energy. Zhang et al. (2013) provided evidence of the beneficial impacts of Fe and Sn nano-particles added to multialkylated cyclopentanes in a vacuum ambient to improve tribological performance. Selimefendigil and Bingolbali (2019) carried out an experimental investigation on doping TiO_2 nano-particles in the compressor oil of a refrigeration system using R134 in order to analyze COP at different nanoparticle fractions. They deduced that adding 1% of nano-particles to compressor oil provides a 21.42% increase in COP.

This study presents improvement of performance of a vapor compression refrigeration system (VCRS) by adding TiO_2 nano-particles to both the compressor lubricant and R134a refrigerant (nano-refrigerant) to make a comparison in terms of cooling and tribological performance with the neat R134a and POE. The performance parameters considered in this study include temperature drop across the condenser and gain across the evaporator, cooling time, energy consumption, compressor suction-discharge pressure and temperature, COP, average coefficient of friction (μ_a) and wear rate (ψ). TiO_2 nano-particles were chosen as nano-additive due to their strong thermophysical and anti-oxidant properties, low toxicity, pleasant odor and non-volatility (Johnson et al. 2013; Tuszynski et al. 2014). The stability of the nano-fluids should be well analyzed (not standardized yet) due to importance of making homogeneous mixture

which has substantial effect on cooling performance and long service life of the compressor mechanism. In this context, DLS analysis was established which is not a common research in relevant studies. Furthermore, to the authors' knowledge, no study has been conducted related to incorporation of TiO_2 nano-particles in both refrigerant and compressor lubricant (at the same time) along with thorough cooling performance, thermos-gravimetric and tribological analyses. Relevant researches (i.e., the above-mentioned references) often concentrate solely on increasing COP by the addition of nano-particles to the compressor lubricant or refrigerant whereas this study explains the effectiveness of a refrigeration system (theoretically and experimentally) charged with various nano-fluids in terms of both cooling performance and tribological improvement. Thus, this study is expected to be a good guide for enhancing effectiveness of cooling systems.

2 Experimental Procedure

2.1 *Thermal Stability Analysis of TiO_2 Nano-Particles*

The tribological features of mechanical systems are significantly influenced by the geometry and dispersion of the nano-additive inside the structure. For instance, the rolling effect, which facilitates a reduction in contact areas and wear, can be effectively achieved by the sphere-like form of the nano-additive (Kreivaitis et al. 2013). Therefore, it is crucial to conduct morphological analysis in order to examine the geometry and/or particle clustering within the nanoparticle's self-structure. TiO_2 nano-particles (~55 nm) in the structure itself have a sphere-like shape and uniform dispersion, as seen in Scanning Electron Microscopy (SEM) images (Fig. 1). Thermo-gravimetric techniques reveal details regarding how the temperature effect alters the structure of nano-particles. Endothermic peaks indicate phase shifts, dehydration, degradation and reduction reactions, whereas exothermic peaks typically depict chemical reactions, polymerization, or crystallization processes. A high level of thermal stability, or the absence of peaks, means that the sample does not degrade while being worked on in that temperature range (Peng et al. 2007; Zin et al. 2014; Kamal et al. 2016). Thermal stability characteristics of the TiO_2 nano-particles in the temperature range of 25–1000ºC was investigated via differential scanning calorimeter (DSC) and thermo-gravimetric analysis (TGA) devices (Table 1).

2.2 Nano-Fluid Preparation

TiO_2 nano-particles with a mass purity rate of 99.7% were dispersed in the R134a refrigerant (nano-refrigerant) and

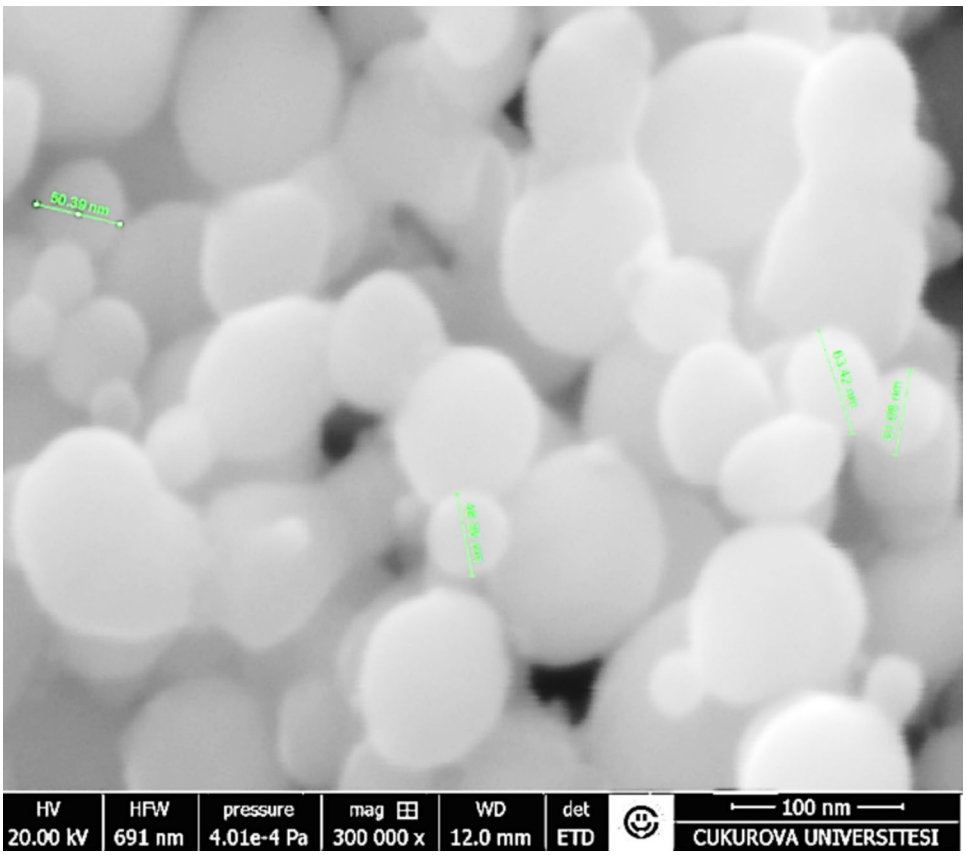


Fig. 1 SEM images of the TiO_2 nano-particles

Table 1 Technical specifications of the thermal stability determination devices

DSC		TGA	
Operating temp	− 170–1000 ℃	Operating temp	25–1600 °C
Temp. accuracy	± 0.2 ℃	Heating rate	0.02–150 K/min
Temp. resolution	± 0.02 ℃	Measurement capacity	Max. 1 g
Heating rate	300 ℃/min @ 0.02 ℃	Balance precision	0.1 µg
Measurement range	± 350 mW	Max. sample volume	< 900 µL
Calorimeter sensitivity	0.02 µW		

Table 2 Specifications of the DLS device

Particle diameter measurement capacity	3.8–100 µm
Z-p mobility	± 20 µcm/Vs
Measurement sensitivity	± 2 mV
Laser	He–Ne
Laser wavelength	633 nm (for this study)
Detection angle	173° (for this study)

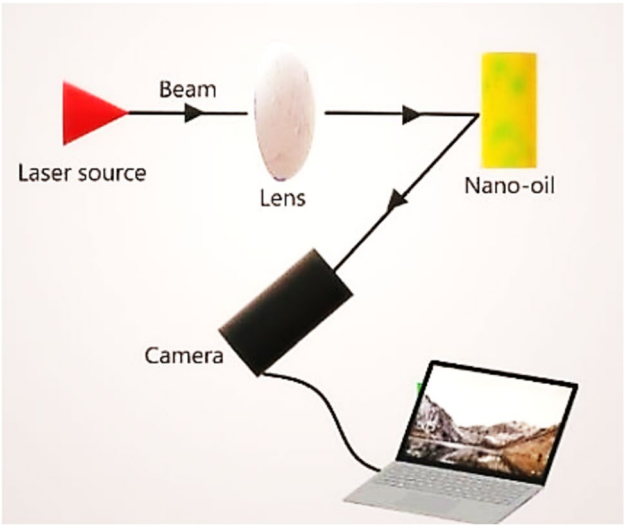


Fig. 2 Illustration of DLS device

compressor's POE (nano-lubricant) at fractions of 0.1 vol% and 0.5 vol% separately. R113 can be utilized as the host fluid to create a nanofluid with well-dispersed nanoparticles (Alawi et al. 2014; Peng et al. 2009b). Thus, initially, nano-particles were added to a negligible amount (10 g) of R113 as host fluid due to maintaining its liquid state at experimental conditions as the R134a would be in vapor state at room temperature and atmospheric pressure. The nano-lubricant suspensions were prepared by directly including nano-particles in the lubricant (liquid state at designated conditions). The nano-fluids underwent 1.5 h of sonication (0.25% kW and 44 kHz) after 1 h of magnetic stirring. The ultra-sonicated nano-particles in R113 was then fed to the formerly R134a charged system. To avoid any potential detrimental effects on the thermo-physical properties of the refrigerant, the nano-lubricants were prepared without any modifications. In the vapor compression refrigeration system, the phase shift of nano-particles and refrigerant combination occurs as it passes through the compressor, evaporator, condenser, and expansion valve. The lack of standardization in the process of combining nano-particles with a refrigerant has an impact on the refrigeration system's thermal performance. Therefore, the cooling performance of the system can be adversely affected by high sedimentation, and the tribological performance characteristics of the system are significantly influenced by the good dispersion of the nano-particles in the lubricant. Moreover, agglomeration on the contacting surfaces of the compressor mechanism could result in an increase in the rate of friction-wear. Thus, it is important to observe the dispersion characteristics of nano-particles in nano-fluids (Guoliang et al. 2009). Based on this idea, the lubricant's nanoparticle dispersion characteristics were determined using the dynamic light scattering (DLS) (Table 2). For determining in situ the sizes, size distributions, and (in some situations) the shapes of nano-particles in liquids, DLS is one of the most adaptable and practical methods. The device is designed to measure size distributions, dispersion (an electrokinetic phenomenon of sedimentation potential), and, in certain situations, the shapes of dry and powdered nano-particles in liquids. It operates at a specific wavelength and a detection angle (Pecora 2000; Murdock et al. 2008). It is comprised of a laser source, lens and a photodetector. The beams scattered from the nano-particles are sensed by a detector once the laser is directed onto the nano-lubricant, and related data are then collected by a data acquisition system to be processed via a special software (Fig. 2). The well-known Rayleigh equation quantifies the dispersed light intensity (Γ) of a spherical particle of which size is substantially smaller than the input light's wavelength (Λ) (Vysotskii et al. 2009):

$$\Gamma = I_0 \frac{9\pi^2 V^2}{2r^2\Lambda^4}\left(\frac{\Phi^2-1}{\Phi^2+2}\right)^2\left(1+\cos^2\beta\right) \quad (2)$$

where "I_0" is incident light intensity, "V" is particle volume, "r" is the distance between the point of observation and the particle, "Φ" is particle to medium refractive index ratio, "β" is the angle between the directions of the incident and the scattered lights.

Zeta potential (Z-p), is a parameter that describes the electrical potential of a plane on which a particle travels and it offers details about the suspension stability including particle agglomeration and complexation of nano-particles. The Hückel equation can be utilized to calculate Z–p for particle sizes smaller than 100 nm (Delgado et al. 2007; Xu 2008):

$$Z - p = \frac{3\eta * \upsilon}{2\varepsilon * \varepsilon_0} \tag{3}$$

where "υ" is the electrophoretic mobility, "η" is the liquid viscosity, "ε" is the dielectric constant and "ε_0" is the permittivity of free space.

2.3 Refrigeration System Test Rig

The refrigeration test rig (Fig. 3) used in this study comprises of a hermetically sealed reciprocating compressor, an air-cooled condenser, an expansion valve and an evaporator (Table 3). The first step was to eliminate moisture and vacuum the refrigeration system via an air compressor. The VCRS was turned ON to reach its steady condition referring to data sheet of the system (considering experimental ambient conditions) as shown in Table 4 after being charged with 140 g of R134a refrigerant. Following confirmation of the steady state, temperature and pressure readings were taken at the compressor's discharge and suction, condenser output, and evaporator input, in every 10 min. Thermocouples and pressure gauges were

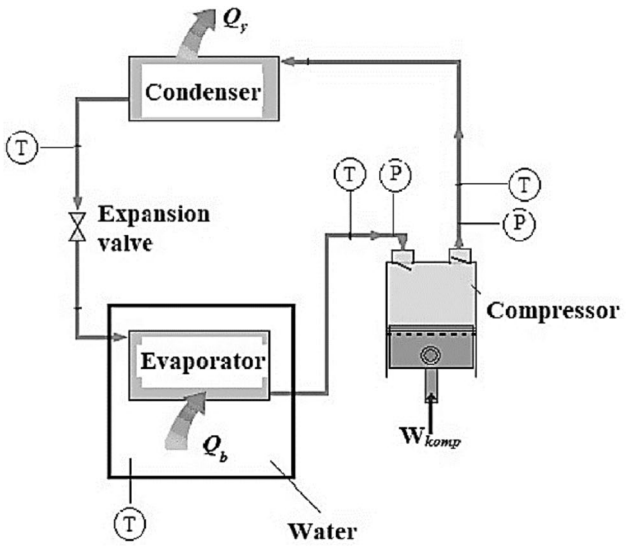


Fig. 3 Schematic of the VCRS

Table 3 VCRS specifications

System pipe diameter	10 mm
Evap. and cond. tube diameter	7 mm
Evaporator water capacity	25 L
Refrigerant capacity	140 g
Reciprocating compressor power	0.18 kW (hermetically sealed)
Pressure gauge	±0.5 kPa with 0–700 bar range
Thermocouples	K-type ± 0.2 °C with− 20–250 °C range
Energy meter	3200 Imp./kWh, 10 pulse-measurement with 0.01 s accuracy

installed on the thermally insulated pipe walls to increase measurement reliability. The flow rate of the refrigerant was maintained at 6 L/h under the control of a rotameter with a measurement range of 0–40 L/h. The evaporator unit was submerged in a water-filled container and energy consumption of the refrigeration system was obtained via an energy meter (range: 0–20 A) connected to the compressor. In order to evaluate heat release rate (q in kW), the following factors were taken into account: "m" mass of water (kg); "c" specific heat capacity (J/kg °C); "K" energy meter constant (impulse/kWh); "n" number of pulses taken in energy meter; "ΔT" temperature difference for the cooled water in the evaporator (°C); and the time lapse, "t" to reduce the T_1 to T_2. In each experimental trial, the water was maintained at about ambient temperature of 25 ºC (T_1) and observations were made until the temperature of the water was reduced to about 10 ºC (T_2). Cooling performance of the system (discussed in the next related section) was also analyzed considering related parameters of COP, cooling time analysis, temperature drop across condenser, temperature gain across evaporator, heat transfer coefficient calculations for both condenser and evaporator.

$$q = \frac{m * c * \Delta T}{t} \tag{4}$$

$$CW = \frac{3600 * n}{t * K} \tag{5}$$

Table 4 VCRS steady state conditions (average)

Compressor suction temperature	30 °C
Compressor discharge temperature	55 °C
Compressor suction pressure	~2 bar
Compressor discharge pressure	5.5 bar
Evaporator inlet temperature	− 3.5 °C
Condenser outlet temperature	51 °C

$$COP = \frac{q}{CW} \tag{6}$$

The following equations were to be used to determine the absolute errors for the directly measured quantities considering maximum of the measured parameter (ξ_{max}), percentage error (Σ) and measurement range (ℓ) (Sanukrishna et al. 2017):

$$\Delta\xi_{max} = \pm(0.3 + 0.5\xi_{max}) \tag{7}$$

$$\Sigma(\%) = (\Delta\xi_{max}/\ell) \times 100 \tag{8}$$

The uncertainty of COP can be determined using propagation of error approach and estimated relative uncertainty of the COP can be found using Eqs. (9) and (10), respectively (Taylor and Kuyatt 1994; Messerly 2016):

$$\sigma(COP) = \left[\left(\frac{\partial COP}{\partial q}\right)^2 \sigma(q)^2 + \left(\frac{\partial COP}{\partial CW}\right)^2 \sigma(CW)^2\right]^{1/2} \tag{9}$$

Table 5 Error data

Parameter	Error (%)
Temperature	~0.4
Pressure	~5.9
Coefficient of friction	~0.45
Coefficient of performance	~0.8
Heat release rate	~0.2
Compressor work	~3

$$\frac{\sigma(COP)}{COP} = \left[\left(\frac{\sigma(q)^2}{q^2}\right) + \left(\frac{\sigma(CW)^2}{CW^2}\right)\right]^{1/2} \tag{10}$$

Here, $\sigma(COP)$ and $\sigma(CW)$ represent the standard deviation and standard error can be found considering number of data taken. Table 5 displays the estimated error statistics based on the devices' measurement range and error as well as computed values based on the test trials.

2.4 Tribological Tests

The metal samples cut from the spare piston ring of the VCRS compressor underwent friction process via a linear (reciprocating) tribotester as illustrated in Fig. 4 to mimic the compressor mechanism. The tribological analyses were conducted at room temperature of 20–25 °C and relative humidity of 55–60%. A steel ball (100Cr6) with a diameter of 5 mm was used as a scratcher on the sample surface, moving 400 m per minute at a linear sliding speed of 2400 mm/min under normal load of 20 N and a stroke of 4 mm. As the scratcher begins the reciprocating motion on the sample surface, related data were collected via a logger and transferred to a special software to compute the coefficient of friction (μ) by dividing the normal load by the shear force between the friction pairs. The friction tests were conducted on identical metal samples fixed onto the oil vessel and submerged in 120 mL of nano-lubricant of POE + 0.1vol% TiO_2 (P0.1) and POE + 0.5vol% TiO_2 (P0.5). Each experiment was carried out at 60 °C oil temperature (average functioning condition of the mechanism). Average of the coefficient of friction (μ_a) was taken into account to improve the accuracy. The worn surfaces of the samples were examined in the next stage of tribological analysis. To determine the weight loss of the

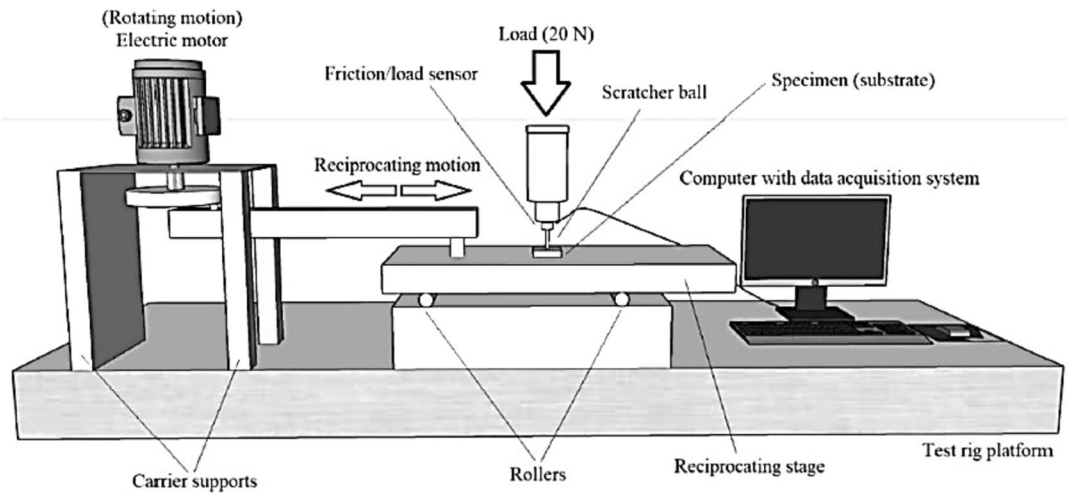


Fig. 4 Illustration of the linear tribotester

samples subsequent to friction analysis, each specimen was first weighed using a precise digital balance before and after the tests. However, in terms of tribological performance of nano-lubricant, wear rate (ψ) gives more accurate results than weight losses as it encompasses more parameters and can be computed using Eq. (11) (Zhang et al. 2019):

$$\psi = \frac{A * L}{F * \ell} \tag{11}$$

where "A" is the trace area (mm^2), "L" is the amount of reciprocating motion (mm), "F" is normal load (N), "ℓ" is sliding distance (m).

SEM and AFM analyses were utilized to visualize the morphology of the worn surfaces. After friction tests, the presence of the nano-particles on the wear scar was demonstrated using an energy-dispersive X-ray (EDX) spectrometer.

3 Results and Discussion

3.1 Thermo-Gravimetric Analysis

Thermogravimetric techniques offer insights into how temperature affects the structure of nanoparticles. Endothermic peaks indicate phase shifts, dehydration, degradation, and reduction reactions, whereas exothermic peaks typically depict chemical reactions, polymerization, or crystallization processes. The lack of peaks signifies a high level of thermal stability, meaning that the sample does not degrade while being worked on at that temperature range (Ali et al. 2016; Peng et al. 2007; Zin et al. 2014). Based on the DSC-TGA results, TiO_2 nano-particles showed almost no signs of breakdown and retained their heat stability (no phase change, such as melting or decomposition) until 1000 °C. Only a little sharp peak was observed at around 325 °C in DSC, where the phase transition was barely noticeable addressing an ignorable phase change (Fig. 5). As a result, it may be concluded that TiO_2 nano-particles are capable of preserving their thermal stability even at extreme temperatures.

Table 6 Ζ–p values of nano-fluids with different concentrations (10 days after preparation)

Suspensions	Code	Average zeta-potential (mV)
R134a + TiO_2 (0.1 vol%)	**R0.1**	**69**
R134a + TiO_2 (0.5 vol%)	R0.5	65
POE + TiO_2 (0.1 vol%)	**P0.1**	**62**
POE + TiO_2 (0.5 vol%)	P0.5	57

Bold indicate the results show that Ζ–p of nano-lubricant drops dramatically as of 0.5 vol% TiO_2 concentration and both nano-fluids with 0.1 vol% depicted higher Ζ–p values. Thus, TiO_2 nanoparticles with fraction of 0.1 vol% was chosen as suitable amount for both refrigerant and lubricant

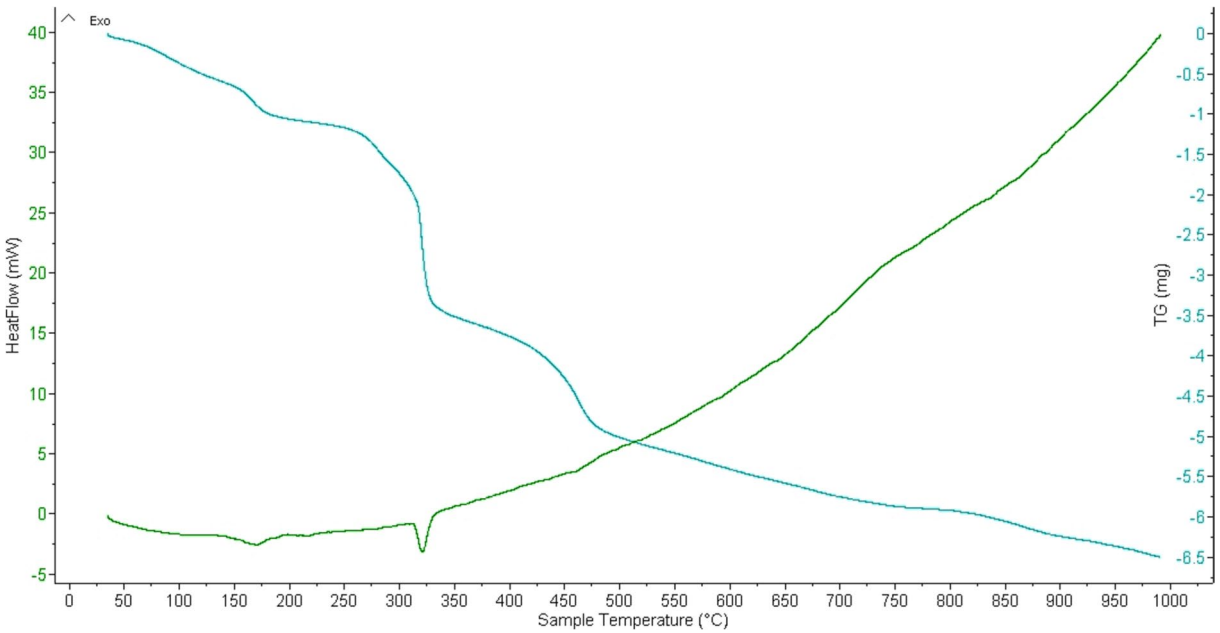


Fig. 5 Thermal stability characteristics of TiO_2 nano-particles

3.2 Nano-Particle Dispersion in Nano-Fluids

The results of the DLS analysis present that, even 10 days after preparation, the average Z–p values of the TiO_2 nano-fluids were within acceptable limits (Table 6), given that a stable suspension for dispersion in liquids with low ionic strength is defined as having a value greater than 30 mV (Sabareesh et al. 2012). Nonetheless, due to possible sedimentation in the nano-lubricant, the Z-p values of the two suspensions were prone to drop as the concentration of nano-particles was increased. The use of surfactants, a common approach for suspension stability, was not employed to impede froth and the degradation of the refrigerant's thermal stability. The results show that Z–p of nano-lubricant drops dramatically as of 0.5 vol% TiO_2 concentration and both nano-fluids with 0.1 vol% depicted higher Z–p values.

3.3 VCR System Analyses

3.3.1 Suction-Discharge Characteristics

The efficiency of a positive displacement compressor directly relates to suction-discharge parameters such as temperature and pressure. Thus, it would be prudent to observe these parameters to better understand the influence of nano-particle incorporation in system fluids. Figure 6 displays the suction and discharge pressure variation of the compressor separately running on POE, P0.1 and P0.5 along with R134a, R134a + 0.1vol% TiO_2 (R0.1) and R134a + 0.5vol% TiO_2 (R0.5). Observations demonstrated that the system comes to steady state as of the 100th minute and adding nano-particles to both compressor's lubricant and refrigerant generally yields the suction and discharge pressures to drop compared to that of pure POE. The mean reductions in suction pressure with nano-fluid combinations compared to non-doped fluid (R134a + POE) are as follows: 6.07% (R0.1 + P0.5), 12.70% (R0.1 + P0.1), 28.36% (R0.5 + P0.1). The mean reductions in discharge pressure with nano-fluid combinations compared to non-doped fluid are as follows: 3.46% (R0.1 + P0.5), 6.02% (R0.1 + P0.1), 8.56% (R0.5 + P0.1). It can be explained by the fact that some lubricant mixes with the refrigerant as it passes through the system. The mixing phenomena raises the viscosity of the refrigerant and lowers the suction-discharge pressure values. Increased viscosity causes reduction in maximum efficiency of the compressor due to higher friction

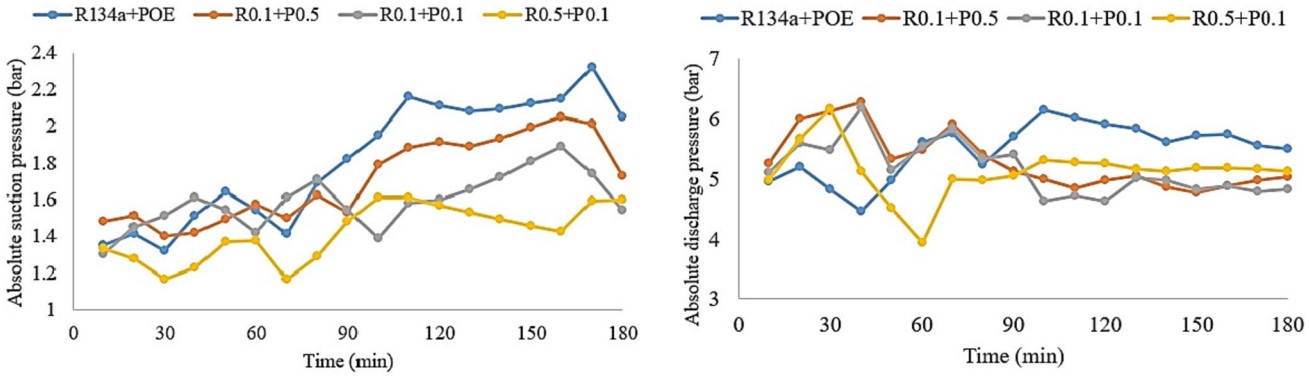


Fig. 6 Compressor suction and discharge pressure vs. test duration

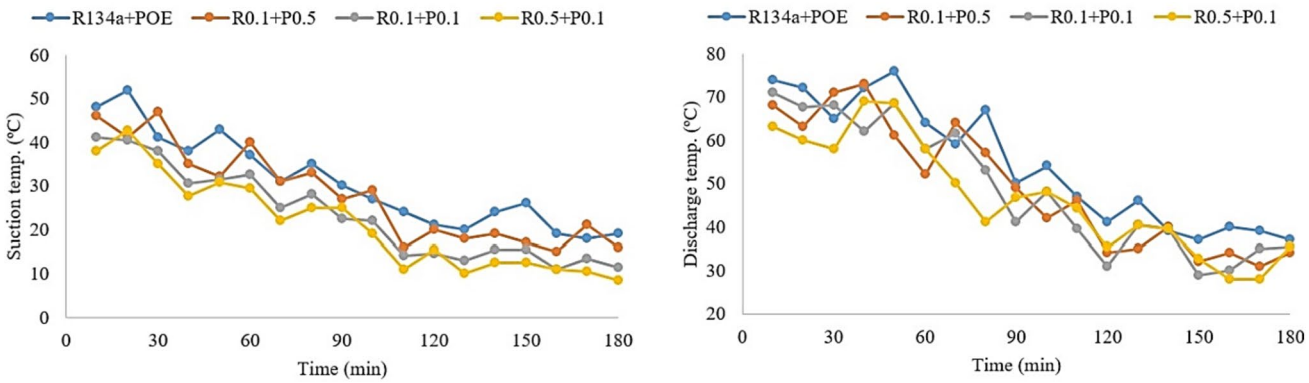


Fig. 7 Compressor suction and discharge temperature vs. test duration

losses at higher viscosities (Abazariyan et al. 2018). The viscosity increment was more dominant for R0.5 + P0.1 than those of the others.

Suction-discharge temperature variation of the compressor with nano-fluid combinations is shown in Fig. 7. Similar to pressure data, suction and discharge temperatures were prone to decrease with comparison to the operation of the system using R134a + POE. The reductions in average suction temperatures were 9.55% for R0.1 + P0.5, 10.29% for R0.1 + P0.1 and 13.61% for R0.5 + P0.1. It can be attributed to the fact that the highest TiO_2 concentration of R0.5 + P0.1 among others provided enhancement in heat transfer throughout the refrigeration system.

3.3.2 Cooling Performance

One of the cooling performance parameter is the length of time it takes to produce the required temperature decrease in water from T_1 to T_2. Figure 8 displays the cooling curves for the temperature reduction from 25 °C to 10 °C at an ambient temperature of about 25 °C and refrigerant flow rate of 6 L/h. The shortest time taken to diminish the water temperature from 25ºC to 10ºC was 2.24 h for R0.5 + P0.1 corresponding to a 22.25% decrease compared to that of R134a + POE. High thermal conductivity of TiO_2 nano-particles provides improved heat carrying capacity and the highest concentration of TiO_2 in R0.5 + P0.1 led to the highest improvement in heat rejection rate among others.

Temperature drop and gain characteristics across condenser and evaporator are of great importance to understand the cooling performance of the VCR system charged with 4 different fluids. The required equations used in this experimental study are presented below (Kundan 2021):

$$Q_c = \dot{m}_{(R0.1-0.5)} * c_{p(R0.1-0.5)} * (T_{in} - T_{out}) \tag{12}$$

where; Q_c: heat released across the condenser; R0.1–0.5: nano-refrigerant with 0.1 vol% and 0.5 vol% TiO_2; $T_{in\text{-}out}$: condenser inlet-output temperature; $m_{(R0.1-0.5)}$: mass flow of the nano-refrigerants; $c_{p(R0.1-0.5)}$: specific heat of the nano-refrigerants

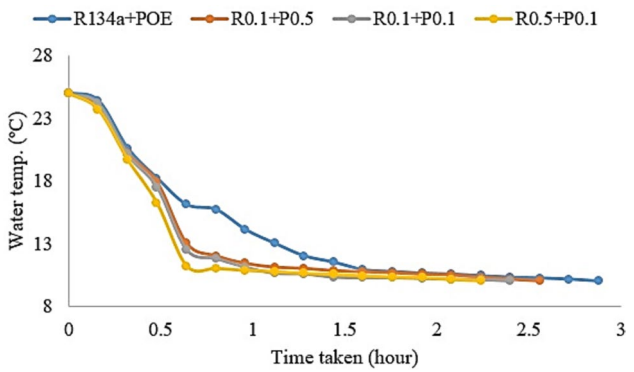


Fig. 8 Time taken to drop water temp. from 25 °C to 10 °C

$$m_{R0.1-0.5} = V_{R0.1-0.5} * \rho_{R0.1-0.5} \tag{13}$$

$$\rho_{R0.1-0.5} = \tau\rho_p + (1-\tau)\rho_{R134a} \tag{14}$$

$$c_{p(R0.1-0.5)} = \tau c_p + (1-\tau)c_{p(R134a)} \tag{15}$$

where V: volume; ρ_p: nanoparticle density; τ: sphericity (equals to 1 for sphere)

$$h_{R134a} = \frac{Q_m}{A * LMTD} \tag{16}$$

$$LMDT = \frac{(T_{h_i} - T_{c_o}) - (T_{h_o} - T_{c_i})}{\ln\left(\frac{T_{h_i} - T_{c_o}}{T_{h_o} - T_{c_i}}\right)} \tag{17}$$

where h_{R134a}: heat transfer coefficient of pure refrigerant; Q_m: mean heat flux; A: related heat transfer area; LMDT: logarithmic mean temp. difference; h_i: hot inlet; c_o: cold outlet

$$k_{(R0.1-0.5)} = \left[\frac{k_p + (n-1)k_{R134a} - (n-1)\beta(k_{R134a} - k_p)}{k_p + (n-1)k_{R134a} + \beta(k_{R134a} - k_p)}\right]k_{R134a} \tag{18}$$

where k_p, k_{R134a}: thermal conductivity of nano-particles and pure refrigerant; $n = 3/\beta$: empirical shape factor

$$Nu_{R0.1-0.5} = \frac{h_{(R0.1-0.5)}D}{k_{(R0.1-0.5)}} \tag{19}$$

$$Nu_{R0.1-0.5} = 0.0059\left\{1 + 7.6286\beta^{0.6886}[Pe_{(R0.1-0.5)}]^{0.001}\right\} [\mathrm{Re}_{(R0.1-0.5)}]^{0.9238}[\mathrm{Pr}_{(R0.1-0.5)}]^{0.4} \tag{20}$$

$$\mathrm{Re}_{(R0.1-0.5)} = \frac{\rho_{R0.1-0.5} * u_m * D}{\eta_{R0.1-0.5}} \tag{21}$$

$$Pe_{(R0.1-0.5)} = \frac{u_{(R0.1-0.5)}}{D_{(R0.1-0.5)}\alpha_{(R0.1-0.5)}} \tag{22}$$

$$\mathrm{Pr}_{(R0.1-0.5)} = \frac{\eta_{(R0.1-0.5)}c_{p(R0.1-0.5)}}{k_{(R0.1-0.5)}} \tag{23}$$

$$\eta_{(R0.1-0.5)} = (1 - 7.3\beta + 123\beta^2)\eta_{R134a} \tag{24}$$

$$\alpha_{(R0.1-0.5)} = \frac{k_{(R0.1-0.5)}}{\rho_{(R0.1-0.5)} c_{p(R0.1-0.5)}} \quad (25)$$

where Nu: Nusselt number; Pe: Peclet number; Re: Reynolds number; Pr: Prandtl number; u_m: mean nano-ref. velocity; D: pipe diameter; u: fluid velocity; $D_{(R0.1-0.5)}$: diffusivity; η: fluid viscosity; α: thermal diffusivity.

Increase rates in temperature drop were found to be 2.96%, 6.95% and 9.05% for R0.1 + P0.5, R0.1 + P0.1 and R0.5 + P0.1, respectively. The addition of TiO_2 nano-particles to R134a refrigerant and POE lubricant boosted the rate of heat transfer across the condenser, causing the refrigerant to sub-cool and further enhancing the system's refrigeration effect. Among nano-fluid combinations, R0.5 + P0.1 gave the best result accounting for a maximum reduction in temperature across the condenser. Lower zeta potential values of nano-fluid combinations with 0.5 vol% TiO_2 depict a probable reduced dispersion of nano-particles in both R134a and POE which may have led to some sedimentation in the suspension and caused diminished heat transfer rate. On the other hand, thanks to improved heat transfer rate due to TiO_2 metal nano-particles, all nano-fluid combinations presented higher temperature drop across condenser when compared to that of R134a + POE.

Temperature gain across the evaporator with various nano-fluids is another parameter to understand the cooling effectiveness of the system. Once the similar calculations were made utilizing related equations given above, enhancements in temperature gain across the evaporator were found to be 4.16%, 9.24% and 13.64% for R0.1 + P0.5, R0.1 + P0.1 and R0.5 + P0.1, respectively while the other conditions were kept same with the tests relating the condenser temperature drop. A greater amount of heat is effectively transferred from the medium to be cooled to the refrigerant passing through the evaporator when nano-particles are added. On the other hand, compressor work was found to be reduced due to improved tribological performance of the reciprocating compressor mechanism thanks to TiO_2 nano-particles dispersed in the POE lubricant. Comparing with 0.1 vol% of TiO_2 in nano-fluids, 0.5 vol% of TiO_2 in R134a gave better results in terms of heat transfer performance (increased heat release rate). On the other hand, the same amount of TiO_2 in POE seems to be partially agglomerated in the lubricant causing increased friction between piston ring and cylinder liner causing increased compressor work (lower COP). Thus, as expected, maximum COP (35.86% increment) was achieved with R0.5 + P0.1 combination. Further discussions about tribological performance will be made in the next section. Figure 9 demonstrates the COP variation with various nano-fluids based on the mathematical and experimental data related to evaporator parameters and power consumption of the compressor.

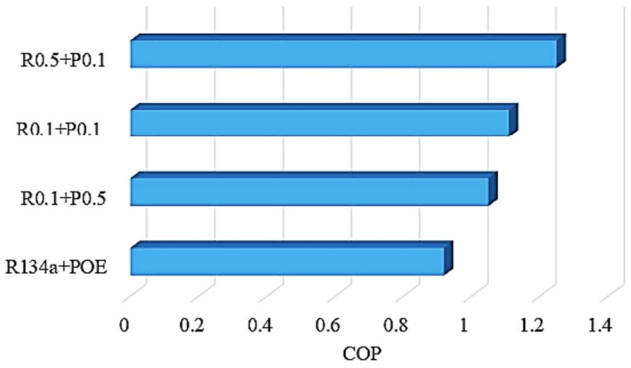


Fig. 9 COP vs. nano-fluid combinations

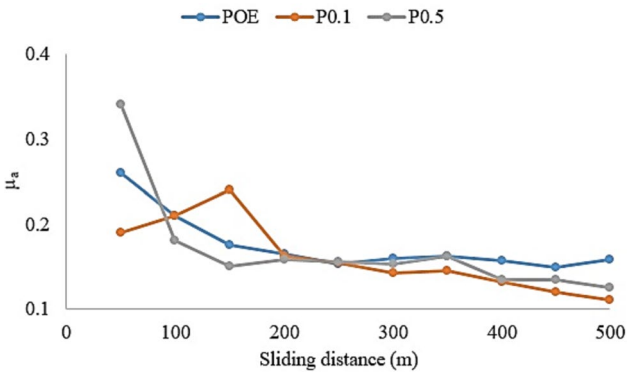


Fig. 10 μ_a vs. sliding distance

3.4 Tribological Analysis

Reducing contact surfaces (rolling effect) or surface roughness (polishing effect) can both lessen friction between two solid surfaces. Average coefficient of friction (μ_a) between the fretting pairs (compressor piston ring-cylinder liner) is to be analyzed to observe the nano-particle effect in the POE lubricant of the compressor. The piston ring samples that were cut from the spare piston rings of the compressor mechanism underwent friction tests while immersed in 120 mL of P0.1 and P0.5 separately. Three tests were conducted on each sample and average of the friction data was taken into consideration to minimize experimental error. The normal load was exerted onto the sample surfaces as to cover scratcher sliding distance of about 500 m. In Fig. 10, mixed lubrication (transition from boundary to hydrodynamic) can be observed until approximately sliding distance of about 250 m. As of 250 m, hydrodynamic friction occurs due to increase in shear stress arising from high scratcher velocity at mid-strokes (mid-sliding distance). The reductions in average coefficient of friction were to be 3.15% and 8.02% for P0.5 and P0.1, respectively compared to that of pure POE. The sphere like particle geometry of TiO_2 (Fig. 1)

facilitates rolling effect resulting in reduced contact surface between the friction pairs. Nano size of the particles provided filling of the grooves on the piston ring and the cylinder liner providing a smoother surface (polishing effect). Furthermore, better dispersion of nano-particles in P0.1 than that of P0.5 (see Table 4) yielded lower friction and reduced compressor work to overcome the friction forces. Since zeta potential of P0.1 is higher than P0.5, it can be concluded that not all of the nano-particles in the lubricant dispersed homogeneously leading to a precipitation and partially increased friction force between the rings and the cylinder liner.

The SEM images of the worn surfaces are shown in Fig. 11. The use of nano-particles clearly reduced the depth of worn tracks. In comparison to neat POE oil bath, the scars on the specimens' surface subsequent to their immersion in P0.1 and P0.5 were smoother than those of POE. This phenomenon can be attributed to lower μ_a values obtained in nano-lubricant ambients compared to neat POE. Additionally, the TiO_2 nano-particles' strong thermal stability (see Fig. 5) paved the way for the preservation of the sphere-like geometry leading to improved rolling effect between the interaction surfaces. Another possibility for the decreased wear tracks can be ascribed to filling of TiO_2 nano-particles into the grooves yielding low surface roughness during the abrasion tests.

The analysis on the worn surface (AFM) in the P0.5 ambient shows that the wear test machine's cutting tool created sharp cutting tracks, whereas transition zones rather than sharp edges were seen on the surfaces worn in P0.1 (Fig. 12). Furthermore, the amount of lost material on the sample surfaces seems to be the lowest for P0.1 compared to P0.5 considering the average height of the sample surface after the friction tests, that is, the wear rates on the surface were lower for the sample immersed in the P0.1. The surface roughness is also higher for P0.5 compared to that of P0.1. The probable precipitation of the TiO_2 nano-particles in P0.5 caused an increase in the friction forces (as confirmed by the zeta-potential, μ_a, COP analyses, etc.) and higher wear rates were observed compared to that of the P0.1. However, both P0.5 and P0.1 gave better results in terms of wear rate when compared to those of POE. The computed wear rate results based on the Eq. (10) are presented in Table 7.

The EDX analysis validates the existence of the nano-particles even after the abrasion tests as shown in Table 8 and 9. A tribo-layer comprised of the nano-particles was formed on the contact surfaces, as confirmed by the chemical composition analysis. The element of Ti in EDX analysis indicates that the tribo-layer on the surface was not totally worn even after the frictions tests.

4 Conclusions

There were clear improvements in terms of cooling and tribological performances of a VCR system running on TiO_2 nano-refrigerant and TiO_2 nano-lubricant after a thorough experimental investigation. All nano-fluids depicted better results when compared to R134a + POE combination. TiO_2 nano-particles preserved their thermal stability up to an average temperature of 1000 °C without any deterioration or decomposition. When the system was charged with nano-fluids, the suction-discharge pressure and temperature values of the compressor were found to be reduced compared to those of the non-doped fluid combination. DLS analysis depicted that the dispersion of the TiO_2 nano-particles in both R134a refrigerant and POE lubricant was in acceptable range even after 10 days of the preparation. However, 0.5 vol% of TiO_2 in

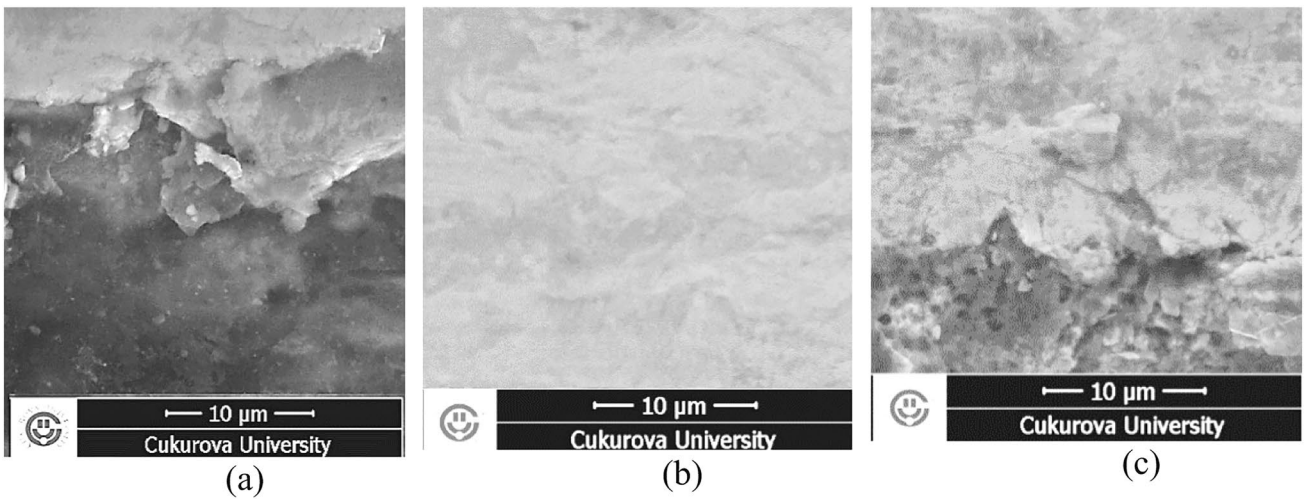


Fig. 11 SEM images of the worn sample surfaces in; **a** POE; **b** P0.1; **c** P0.5

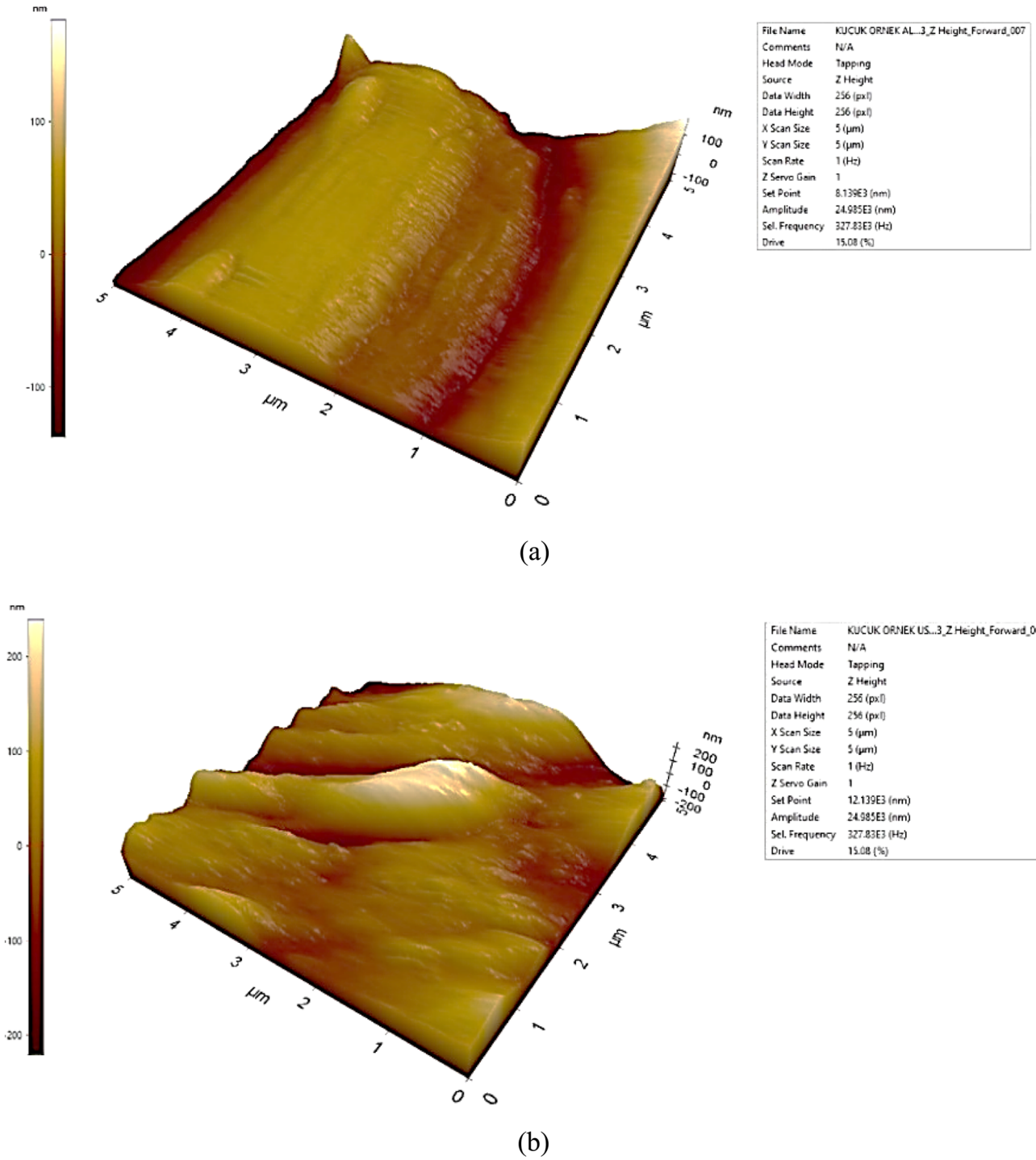


Fig. 12 AFM images of the worn substrates submerged in **a** P0.1 and **b** P0.5

Table 7 Wear rates formed on the samples in different oil baths

Samples immersed in	Wear rate (mm^3/Nm)
POE	34.12×10^{-9}
P0.1	24.21×10^{-9}
P0.5	30.16×10^{-9}

POE showed some challenges due to probable agglomeration in the lubricant leading to increased friction forces (higher compressor work), reduced COP and higher wear rates compared to those of R0.5 + P0.1 and R0.1 + P0.1. The reduction in wear rates were found to be 29.04% and 11.61% for P0.1 and P0.5, respectively compared to that of

Table 8 Chemical constituent of the sample surface after the friction tests in P0.1

Element	Weight %	Atomic %
C K	5.48	20.77
O K	3.85	8.99
Fe K	89.85	68.08
Ti K	**0.82**	**2.16**

Bold indication stands for the existence of TiO_2 nanoparticles in P0.1 even after friction tests

Table 9 Chemical constituent of the sample surface after the friction tests in P0.5

Element	Weight %	Atomic %
C K	9.06	25.26
O K	5.84	14.92
Fe K	84.02	55.86
Ti K	**1.08**	**3.96**

Bold indication stands for the existence of TiO_2 nanoparticles in P0.5 even after friction tests

POE. On the other hand, 0.5 vol% TiO_2 in R134a gave the best results in the terms of cooling and tribological performance with the combination of 0.1 vol% TiO_2 in POE. Heat transfer rate for R0.5 + P0.1 was also found to be the highest among others yielding improved cooling performance. Consequently, it was deduced that R0.5 + P0.1 was the most suitable nano-fluid combination in terms of cooling and tribological performance of the refrigeration system. It is believed that this study will be a good guide for study field of refrigeration in terms of producing more efficient systems with longer service life. Yet, there are issues that should be addressed for future studies such as:

- considering the ideal concentration of various nanoparticles within the base fluid due to the impact of pressure drop caused by greater viscosity of nano-fluids,
- conducting investigations on the proposed correlations of the heat transfer mechanisms and thermo-physical properties,
- requiring additional experimental research on quantum molecular mechanics to enhance the atomic-level chemical interactions,
- general optimization of nano-refrigerants in terms of their shape, size, density, etc. for higher system efficacy.

Acknowledgements The authors would like to thank Cukurova University, Department of Physics and Cukurova University, Central Research Laboratory for their technical support.

Funding This study was fiscally supported by Cukurova University, Scientific Research Projects (Grant number: FBA-2021-14009).

Declarations

Conflict of interest The authors declare no potential conflicts of interest with respect to the research, authorship, and/or publication of this article.

References

Abazariyan S, Rafee R, Derakhshan S (2018) Experimental study of viscosity effects on a pump as turbine performance. Renew Energy 127:539–547. https://doi.org/10.1016/j.renene.2018.04.084

Abolpour B, Shamsoddini R (2023) Multi-objective optimization of nanoparticle mixture for improving the performance of heat exchangers. Iran J Sci Technol Trans Mech Eng. https://doi.org/10.1007/s40997-023-00672-8

Akcay S, Akdag U (2023) Numerical analysis of thermal and hydraulic performance of pulsating nanofluid flow over cam-shaped tube bundles. Iran J Sci Technol Trans Mech Eng 47:969–988. https://doi.org/10.1007/s40997-022-00572-3

Alawi OA, Sidik NAC, Mohammed HA (2014) A comprehensive review of fundamentals, preparation and applications of nanorefrigerants. Int Commun Heat Mass Transf 54:81–95. https://doi.org/10.1016/j.icheatmasstransfer.2014.03.001

Ali MKA, Xianjun H, Bicheng C, Turkson RF, Qingping C (2016) Reducing frictional power losses and improving the scuffing resistance in automotive engines using hybrid nanomaterials as nano-lubricant additives. Wear 364:270–281. https://doi.org/10.1016/j.wear.2016.08.005

Bakthavatchalam B, Habib K, Saidur R, Baran B (2022) Cooling performance analysis of nanofluid assisted novel photovoltaic thermoelectric air conditioner for energy efficient buildings. Appl Therm Eng 213:118691. https://doi.org/10.1016/j.applthermaleng.2022.118691

Choi Y, Lee C, Hwang Y, Park M, Lee J, Choi C, Jung M (2009) Tribological behavior of copper nanoparticles as additives in oil. Curr Appl Phys 9:124–127. https://doi.org/10.1016/j.cap.2008.12.050

Delgado AV, González-caballero F, Hunter RJ, Koopal LK (2007) Measurement and interpretation of electrokinetic phenomena. J Colloid Interface Sci 309:194–224. https://doi.org/10.1016/j.jcis.2006.12.075

Fazlin N, Halim C, Azwadi N, Sidik C (2020) Nanorefrigerants : a review on thermophysical properties and their heat transfer performance. J Adv Res Appl Sci Eng Technol 20:42–50. https://doi.org/10.37934/araset.20.1.4250

Ghalme S, Koinkar P, Bhalerao Y, Ghalme SG (2020) Effect of aluminium oxide (Al_2O_3) nanoparticles addition into lubricating oil on tribological performance. Tribol Ind 42:494–502. https://doi.org/10.24874/ti.871.04.20.07

Ghorbani B, Akhavan-behabadi MA, Ebrahimi S, Vijayaraghavan K (2017) Experimental investigation of condensation heat transfer of R600a/POE/CuO nano-refrigerant in flattened tubes. Int Commun Heat Mass Transf 88:236–244. https://doi.org/10.1016/j.icheatmasstransfer.2017.09.011

Guoliang D, Hao P, Weiting J, Yifeng G (2009) The migration characteristics of nanoparticles in the pool boiling process of nanorefrigerant and nanorefrigerant–oil mixture. Int J Refrig 32:114–123. https://doi.org/10.1016/j.ijrefrig.2008.08.007

Jiang W, Li S, Yang L, Du K (2019) Experimental investigation on performance of ammonia absorption refrigeration system with

TiO_2 nanofluid. Int J Refrig 98:80–88. https://doi.org/10.1016/j.ijrefrig.2018.09.032

Jin Z, Li S, Zhou R, Xu M, Jiang W, Du K (2023) Effects of absorption pressure and temperature on NH_3-H_2O-LiBr-TiO_2 nanofluid absorption performance and system COP. Appl Therm Eng 219:119353. https://doi.org/10.1016/j.applthermaleng.2022.119353

Johnson DW, Bachus M, Hils JE (2013) Interaction between lubricants containing phosphate ester additives and stainless steels. Lubricants 2:48–60. https://doi.org/10.3390/lubricants1020048

Kamal M, Ali A, Xianjun H, Mai L, Bicheng C, Fii R, Qingping C (2016) Reducing frictional power losses and improving the scuffing resistance in automotive engines using hybrid nanomaterials as nano-lubricant additives. Wear 365:270–281. https://doi.org/10.1016/j.wear.2016.08.005

Kane SN, Mishra A, Dutta AK (2016) Preface: international conference on recent trends in physics (ICRTP 2016). In: Journal of physics: conference series 755. https://doi.org/10.1088/1742-6596/755/1/011001

Khan IA, Amirtham VA (2023) Theoretical energy and exergy analysis of flat plate solar collector with TiO_2–Ag/water nanocomposite fluid. Iran J Sci Technol Trans Mech Eng 47:921–939. https://doi.org/10.1007/s40997-022-00565-2

Kong L, Sun J, Bao Y, Meng Y (2017) Effect of TiO_2 nanoparticles on wettability and tribological performance of aqueous suspension. Wear 376:786–791. https://doi.org/10.1016/j.wear.2017.01.064

Kreivaitis R, Padgurskas J, Rukuiza R, Prosyc I (2013) Tribological properties of lubricant additives of Fe, Cu and Co nanoparticles. Tribol Int 60:224–232. https://doi.org/10.1016/j.triboint.2012.10.024

Kumar R, Singh J (2017) Effect of ZnO nanoparticles in R290/R600a (50/50) based vapour compression refrigeration system added via lubricant oil on compressor suction and discharge characteristics. Heat Mass Transf 53:1579–1587. https://doi.org/10.1007/s00231-016-1921-3

Kundan L (2021) Improved performance of a nanorefrigerant-based vapor compression refrigeration system : a new alternative. J Power Energy 235:106–123. https://doi.org/10.1177/0957650920904553

Lee K, Hwang Y, Cheong S, Kwon L, Kim S, Lee J (2009) Performance evaluation of nano-lubricants of fullerene nanoparticles in refrigeration mineral oil. Curr Appl Phys 9:128–131. https://doi.org/10.1016/j.cap.2008.12.054

Li H, Yang W, Yu Z, Zhao L (2015) The performance of a heat pump using nanofluid (R22+TiO_2) as the working fluid–an experimental study. Energy Procedia 75:1838–1843. https://doi.org/10.1016/j.egypro.2015.07.158

Liu Z, Hou G, Taherian H (2022) Techno-economic analysis of Al_2O_3/CuO nanofluid applied in various horizontal ground heat exchangers. Int J Energy Res 46:22894–22912. https://doi.org/10.1002/er.8593

Mahbubul IM, Saidur R, Amalina MA (2013) Heat transfer and pressure drop characteristics of Al_2O_3-R141b nanorefrigerant in horizontal smooth circular tube. Procedia Eng 56:323–329. https://doi.org/10.1016/j.proeng.2013.03.126

Mahbubul IM, Saadah A, Saidur R, Khairul MA, Kamyar A (2015) Thermal performance analysis of Al_2O_3/R-134a nanorefrigerant. Int J Heat Mass Transf 85:1034–1040. https://doi.org/10.1016/j.ijheatmasstransfer.2015.02.038

Messerly RA (2016) How a systematic approach to uncertainty quantification renders molecular simulation a quantitative tool in predicting the critical constants for large n-alkanes. Dissertation, Brigham Young University

Mohamadi S, Yazdi MH, Solomin E, Fudholi A, Sopian K, Chong PL (2021) Heat transfer and entropy generation analysis of internal flow of nanorefrigerant with slip condition at wall. Therm Sci Eng Prog 22:100829. https://doi.org/10.1016/j.tsep.2020.100829

Mohammadi M (2023) Multi-objective shape and flow optimization of finned double-tube heat exchanger filled with nanofluid: a CFD and RSM study. Iran J Sci Technol Trans Mech Eng. https://doi.org/10.1007/s40997-023-00641-1

Mousavi SB, Heris SZ (2020) Experimental investigation of ZnO nanoparticles effects on thermophysical and tribological properties of diesel oil. Int J Hydrog Energy 45:23603–23614. https://doi.org/10.1016/j.ijhydene.2020.05.259

Murdock RC, Braydich-Stolle L, Schrand AM, Schlager JJ, Hussain SM (2008) Characterization of nanomaterial dispersion in solution prior to in vitro exposure using dynamic light scattering technique. Toxicol Sci 101:239–253. https://doi.org/10.1093/toxsci/kfm240

Pecora R (2000) Dynamic light scattering measurement of nanometer particles in liquids. J Nanoparticle Res 2:123–131. https://doi.org/10.1023/A:1010067107182

Peng Y, Hu Y, Wang H (2007) Tribological behaviors of surfactant-functionalized carbon nanotubes as lubricant additive in water. Tribol Lett 25:247–253. https://doi.org/10.1007/s11249-006-9176-7

Peng DX, Kang Y, Hwang RM, Shyr SS, Chang YP (2009a) Tribological properties of diamond and SiO_2 nanoparticles added in paraffin. Tribol Int 42:911–917. https://doi.org/10.1016/j.triboint.2008.12.015

Peng H, Ding G, Jiang W, Hu H, Gao Y (2009b) Heat transfer characteristics of refrigerant-based nanofluid flow boiling inside a horizontal smooth tube. Int J Refrig 32:1259–1270. https://doi.org/10.1016/j.ijrefrig.2009.01.025

Prasad AR, Singh S, Nagar H (2017) A review on nanofluids: properties and applications. Int J Adv Res Innov Ideas Educ 3:3185–3209

Putra N, Roetzel W, Das SK (2003) Natural convection of nanofluids. Heat Mass Transf 39:775–784. https://doi.org/10.1007/s00231-002-0382-z

Sabareesh RK, Gobinath N, Sajith V, Das S, Sobhan CB (2012) Application of TiO_2 nanoparticles as a lubricant-additive for vapor compression refrigeration systems-an experimental investigation. Int J Refrig 35:1989–1996. https://doi.org/10.1016/j.ijrefrig.2012.07.002

Sanukrishna SS, Vishnu AS, Jose PM (2017) Nanorefrigerants for energy efficient refrigeration systems. J Mech Sci Technol 31:3993–4001. https://doi.org/10.1016/j.rser.2010.11.035

Sanukrishna SS, Sha M, Murukan M, Prakash MJ (2019) Effect of SiO_2 nanoparticles on the heat transfer characteristics of refrigerant and tribological behaviour of lubricant. Powder Technol 356:39–49. https://doi.org/10.1016/j.powtec.2019.07.083

Scarpa F, Bianco V (2024) Improving the performance of room temperature magnetic regenerators using Al_2O_3-water nanofluid. Appl Therm Eng 236:121711. https://doi.org/10.1016/j.applthermaleng.2023.121711

Selimefendigil F, Bingolbali T (2019) Experimental investigation of nano compressor oil effect on the cooling performance of a vapor-compression refrigeration system. J Therm Eng 5:100–104. https://doi.org/10.18186/thermal.513023

Shammasi G, Pakravan HA, Emdad H (2023) The superiority of eulerian two-fluid model for simulation of natural convection of nanofluids in comparison with other models. Iran J Sci Technol Trans Mech Eng 47:381–395. https://doi.org/10.1007/s40997-022-00528-7

Sheikholeslami M, Rezaeianjouybari B, Darzi M, Shafee A, Li Z, Khang T (2019) Application of nano-refrigerant for boiling heat transfer enhancement employing an experimental study. Int J Heat Mass Transf 141:974–980. https://doi.org/10.1016/j.ijheatmasstransfer.2019.07.043

Taylor BN, Kuyatt CE (1994) Guidelines for evaluating and expressing the uncertainty of NIST measurement results. NIST Technical Note 1297. https://emtoolbox.nist.gov/publications/nisttechnicalnote1297s.pdf. Accessed 02 Feb 2024

Thottackkad MV, Perikinalil RK, Kumarapillai PN (2012) Experimental evaluation on the tribological properties of coconut oil by the addition of CuO nanoparticles. Int J Precis Eng Manuf 13:111–116. https://doi.org/10.1007/s12541-012-0015-5

Tuszynski W, Szczerek M, Michalczewski R, Osuch-slomka E, Rogos E, Urbanski A (2014) The potential of the application of biodegradable and non-toxic base oils for the formulation of gear oils—model and component scuffing tests. Lubr Sci 26:327–346. https://doi.org/10.1002/ls.1262

Vysotskii VV, Uryupina OY, Gusel'nikova AV, Roldugin VI (2009) On the feasibility of determining nanoparticle concentration by the dynamic light scattering method. Colloid J 71:739–744. https://doi.org/10.1134/S1061933X09060027

Xu R (2008) Progress in nanoparticles characterization: sizing and zeta potential measurement. Particuology 6:112–115. https://doi.org/10.1016/j.partic.2007.12.002

Yang J, Jia J, Li X, Lu C, Feng X (2021) Synergistic lubrication of Ag and Ag_2MoO_4 nanoparticles anchored in plasma-sprayed YSZ coatings : remarkably-durable lubricating performance. Tribol Int 153:106670. https://doi.org/10.1016/j.triboint.2020.106670

Zhang S, Hu L, Feng D, Wang H (2013) Anti-wear and friction-reduction mechanism of Sn and Fe nanoparticles as additives of multialkylated cyclopentanes under vacuum condition. Vacuum 87:75–80. https://doi.org/10.1016/j.vacuum.2012.07.009

Zhang S, Hao Q, Liu Y, Jin L, Ma F, Sha Z, Yang D (2019) Simulation study on friction and wear law of brake pad in high-power disc brake. Math Probl Eng 2019:1–15. https://doi.org/10.1155/2019/6250694

Zin V, Agresti F, Barison S, Colla L, Mercadelli E, Fabrizio M, Pagura C (2014) Tribological properties of engine oil with carbon nanohorns as nano-additives. Tribol Lett 55:45–53. https://doi.org/10.1007/s11249-014-0330-3

Springer Nature or its licensor (e.g. a society or other partner) holds exclusive rights to this article under a publishing agreement with the author(s) or other rightsholder(s); author self-archiving of the accepted manuscript version of this article is solely governed by the terms of such publishing agreement and applicable law.